



## Synthesis, Properties and Effect of Ionizing Radiation on Sorption Behavior of Iron Silico-antimonate

I. M. Ali, E. S. Zakaria, S. A. Shama\* and I. M. El-Naggar

*Hot Labs. Centre, Atomic Energy Authority, P.C. 13759, Cairo, Egypt.*

*\*Chem. Dept., Faculty of Science, Benha Univ., Egypt.*

*E-mail address: ismail\_m\_ali@yahoo.com*

*Received: 26/10/2008. Accepted: 14/12/2008.*

---

### ABSTRACT

Incorporation of iron oxide into silico-antimonate of different Si/Sb molar ratios provides a class of doubly salts ion exchangers of good ion exchange properties. The physico-chemical properties of the prepared materials were determined using XRF, FTIR, TGA/DTA and XRD techniques. Chemical stability, thermal stability, ion-exchange capacity and distribution behaviors have been carried out to understand the ion exchange behavior of the materials. On the basis of distribution studies, the obtained materials were found to be highly sorbents for Sr (II) and Ce (III) ions. Comparison of the diffractograms, thermograms, IR spectra and distribution studies of FeSiSb (114), it was found that  $\gamma$ -irradiation doses (up to 100 kGy) not result any detectable structural changes. Effect of reaction temperatures on the exchange process of both Sr (II) and Ce (III) ions has been investigated and some physical parameters such as  $\Delta H^\circ$ ,  $\Delta S^\circ$  and  $\Delta G^\circ$  were determined.

**Keywords:** Ion Exchange, Iron silico-antimonate, Distribution coefficient, Strontium, Cerium.

---

### INTRODUCTION

Inorganic ion exchangers are in general superior to organic exchangers in some aspects as they are resistant towards high ionizing radiations and can be used at elevated temperatures without being danger of decomposition. Moreover, they often exhibit specificity towards certain metal ions. It is for these reasons that there has been a revolutionary growth in the field of synthetic

ion exchangers. Efforts have been made to improve the chemical, thermal and mechanical stabilities of ion exchangers and to make them highly selective for certain metal ions. It has been observed that double salts often exhibit much better ion exchange properties than do simple salts<sup>1-5</sup>. The synthesis conditions of hydrous metal oxides significantly affect the composition and crystallinity, and thus the ion exchange properties of the product. Quadrivalent metal antimonates e.g. Ti(IV)Sb and Sn(IV)Sb have extensively been studied<sup>6,7</sup>. These materials were typically prepared by precipitation in the hydrolysis reactions of the metals, which produces hydrous oxides of relatively low crystallinity.

Antimony (IV) based ion exchanger have received attention because of their excellent ion exchange behavior<sup>8,9</sup>. In 2003, Moller *et al.*<sup>10</sup> synthesized extensive series of titanium antimonates in various Ti : Sb ratios and it is found that the acidity of the exchangers was increased with increasing Sb<sup>5+</sup> content. The <sup>134</sup>Cs, <sup>85</sup>Sr and <sup>57</sup>Co distribution coefficient ( $K_d$ ) values determined in 0.1M HNO<sub>3</sub> prove that this expectation is correct<sup>10</sup>. On the other hand, double salts comprising molybdsilicate<sup>3</sup>, arsenosilicate<sup>11</sup>, tungstophosphate<sup>12</sup>, and tungstoarsenate<sup>13</sup> based on Sn(IV) have been synthesized. Recently, stannic molybdsilicate was synthesized and the effect of temperature on distribution coefficients of metal ions was studied<sup>3</sup>. In addition, a mixed material of the class of tetravalent bimetallic acid salt zirconium titanium phosphate (ZTP) has been synthesized by the sol-gel technique<sup>14</sup>. The equilibrium exchange of H<sup>+</sup> in ZTP for Mg<sup>2+</sup>, Ca<sup>2+</sup>, Sr<sup>2+</sup> and Ba<sup>2+</sup> ions has been studied at 303-333 K at constant ionic strength.

The present work has been undertaken in an attempt to synthesize a new phases of iron silico-antimonate in two different Sb<sup>5+</sup> contents. Efforts have been made to explore the effect of nitric acid concentration, temperature, ionizing radiation on the distribution coefficients of metal ions.

## EXPERIMENTAL

Reagents and chemicals were analytical grade and used without further purification, <sup>85</sup>Sr and <sup>144</sup>Ce isotopes were purchased from Amersham International.

### *Synthesis of FeSiSb*

For the preparation of iron silico-antimonates, the metal solutions of 0.6M of Na<sub>2</sub>SiO<sub>3</sub> and 0.6M of Fe(NO<sub>3</sub>)<sub>3</sub> were added at the same time in dropwise

with continues stirring to solutions of 0.6M of Sb-metal dissolved in aqua regia in volume percent given in Table 1, respectively. During mixing the appropriate solutions, a fine yellow precipitate was obtained by the time of addition. Stirring was continued for 15 min after addition the reactants. The reaction products was aged to about 5 days in mother solution then decanted and washed several times with bidistilled water at constant pH (about 3) then centrifuged and dried by gentle heating. The products were cracked by hot water (90°C) followed by 0.1M HNO<sub>3</sub> washing to be free from Cl<sup>-</sup> ions and rewashed with bidistilled water to remove nitrate groups. Finally, the brown solids were dried at 70°C in a drying oven, ground, sieved to mesh size 0.225-0.425mm and stored at room temperature.

### ***Characterization of the products***

Powder X-ray diffraction was performed using a Shimadzu X-ray diffract meter; model XD610, with a nickel filter and K<sub>α</sub> Cu radiation (1.54° Å) operating at 30 kV and 30 mA. Thermal analysis was determined using a Shimadzu DT-60 thermal analyzer, Kyoto, Japan. The samples were measured at ambient temperature up to 1000°C with a heating rate of 15 °C /min under nitrogen atmosphere. The FTIR spectra were acquired with a Bomem FTIR spectrometer applying KBr disc technique. The X-ray fluorescence was carried out using Phillips X-ray fluorescence model PW 2400 spectrometer, by applying the pressed technique.

### ***Chemical dissolution***

About 0.3 g portions of FeSiSb (111) and FeSiSb (114) samples were treated with 30 ml each of different acids (HNO<sub>3</sub> and HCl), NaOH and demineralized water (DMW) for 48 h with intermittent shaking. The supernatant liquid was analyzed for Fe(III), Si(IV) and Sb(VI) using ICP<sub>seq</sub>-7500 spectrometer, Shimadzu Model 1200 product, Japan.

### ***Batch distribution studies***

A batch technique was followed to determine the distribution coefficients (K<sub>d</sub>) values of <sup>85</sup>Sr and <sup>144</sup>Ce isotopes (overnight standing sufficient to attain equilibrium) on different product ratios as a function of acid concentrations and V/m is 100 ml/g. The studied ions were determined radiometrically as <sup>85</sup>Sr and <sup>144</sup>Ce isotopes, respectively, using single channel analyzer supplied with a well-

type NaI (TI) detector (UK). Distribution coefficients ( $K_d$ ) were calculated by the relation:

$$K_d = (A_o - A) / A \cdot V/m \quad (\text{ml/g}) \quad (1)$$

where,  $A_o$  is the initial counting rate of considered elements in solution,  $A$  is the final counting rate of the considered element in the solution at equilibrium,  $V$  is the volume of the solution (ml) and  $m$  is the mass of the exchanger (g). The obtained  $K_d$  values indicated the selectivity of the materials for each strontium and cerium ions.

On the other hand, the sorption capacities of the two iron silico-antimonate products for  $\text{Na}^+$  ions were measured by repeated batch equilibration of the samples with the desired solutions at different acid concentrations in a shaker thermostated water bath at  $20 \pm 1^\circ\text{C}$  until saturation was achieved. The capacity may express in terms of the following equations:

$$\% \text{ Uptake} = (A_o - A_e) / A_o \times 100 \quad (2)$$

$$\text{capacity (meq g}^{-1}\text{)} = (\% \text{ uptake} / 100) C_o \cdot Z \cdot V / m \quad (3)$$

where,  $C_o$  is the initial concentration of the ions and  $Z$  is the valance of tested ions. Generally, the experiments showed that the reproducibility limit of measurements agreed to  $\pm 3\%$ .

## RESULTS AND DISSCUSION

### *Characterization of Synthesized materials*

In this work, two samples of glassy brown granules of iron incorporated silico-antimonates were obtained by the precipitation reaction. On the basis of DTA/TG, IR, XRD and XRF measurements, iron silico-antimonate has been obtained in two different structures depending on the Sb contents as given in Table 1. The obtained materials named as FeSiSb (111) and FeSiSb (114) were found to possessed high chemical, mechanical and radiation stabilities. The solubility experiments (Table 2) showed that the materials have reasonable good chemical stability as the results indicated that the materials were resistant to 5 M HCl, 5M $\text{HNO}_3$  and 3M  $\text{H}_2\text{SO}_4$ . No chemical dissolution in DMW and alkaline media. The chemical stability may be due to the presence of binding silico-antimonate which can prevent the dissolution of iron or leaching of any constituent element into the solution. The experiment indicated that higher stability for FeSiSb (114) sample compared to FeSiSb (114) one. Different tools

of physio-chemical analyses (Figs.1-3) indicated obvious structural differences of the two obtained products. The empirical formulas were indicated in Table 1.

**Table 1. Details of precipitation, empirical formulas, characterization and Na<sup>+</sup> capacity (meq /g) of iron silico-antimonates at 25±1°C.**

Exchanger form	$\gamma$ -Dose (kGy)	Reactant volume ratios Fe : Si : Sb	Empirical formula	% water content	XRD	Na <sup>+</sup> exchange capacity
FeSiSb(111)	0	1 : 1 : 1	FeSi <sub>4</sub> Sb <sub>6</sub> O <sub>18</sub> . 18H <sub>2</sub> O	20.23	Am.*	1.16
FeSiSb(114)	0	1 : 1 : 4	FeSi <sub>0.5</sub> Sb <sub>5.5</sub> O <sub>11</sub> .9H <sub>2</sub> O	20.63	Cubic	1.56
FeSiSb(114)	25	1 : 1 : 4	-	20.40	Cubic	1.43
FeSiSb(114)	50	1 : 1 : 4	-	20.25	Cubic	1.40
FeSiSb(114)	100	1 : 1 : 4	-	20.17	Cubic	1.39

**Table 2. Chemical stability of FeSiSb (111) and FeSiSb (114) in various media.**

Medium	Chemical stability, mg/30 ml					
	FeSiSb(111)			FeSiSb(114)		
	Fe	Si	Sb	Fe	Si	Sb
DMW	0.00	0.00	0.00	0.00	0.00	0.00
3 M HCl	0.30	0.10	0.10	0.30	0.10	0.00
5 M HCl	0.50	0.30	0.30	0.40	0.20	0.20
3 M HNO <sub>3</sub>	0.60	0.00	0.20	0.30	0.00	0.10
5 M HNO <sub>3</sub>	0.80	0.20	0.40	0.50	0.10	0.20
3 M H <sub>2</sub> SO <sub>4</sub>	1.00	0.60	0.30	0.50	0.50	0.30
1 M NaOH	0.00	0.00	0.00	0.00	0.00	0.00

The XRD patterns (Fig. 1 a & b) indicated that, completely amorphous structure of FeSiSb (111) while the FeSiSb (114) well coincide with that of cubic structure of antimony oxide crystals (antimonic acid) as indexed and matched from library chards<sup>15</sup>. Examining the peak intensities of FeSiSb(114) as given in Fig. 1 b revealed that trace of cubic structure which means that the crystallinity degree may be depend on the Sb content in the material. Thus, XRD data confirmed that, the antimony is the controlled atom in the FeSiSb structure and the relative crystalline nature belongs to the antimony oxide phase. However, the same result excludes the rule of iron oxide and/or silicate phase as effective components in the cubic structure of FeSiSb (114). Ali *et al.* reported that, most silicates and hydrous iron oxides that obtained by direct precipitation methods are amorphous in nature and have negative effect in crystallinity improvement<sup>16</sup>.

The IR spectra (Fig. 2 a & b) indicated that the absorption peaks related to O-H bonding at  $1640$  and  $3400\text{ cm}^{-1}$  is the main peaks for the two iron silico-antimonates products<sup>17</sup>. Also the IR spectra show strong band at  $1118$  and weak band at  $958\text{ cm}^{-1}$ , which indicates to the presence of silicate and antimonate groups, respectively<sup>17</sup>.

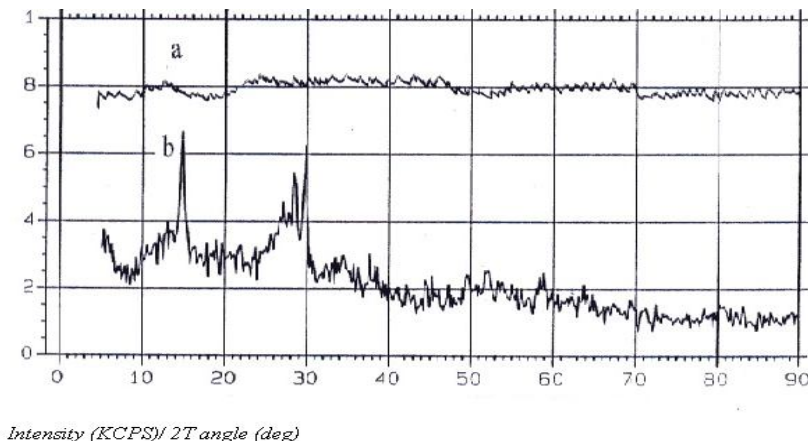


**Fig. 1.** X-ray diffraction patterns of iron silico-antimonate with different antimony contents, FeSiSb-111 (a) and FeSiSb-114 (b).

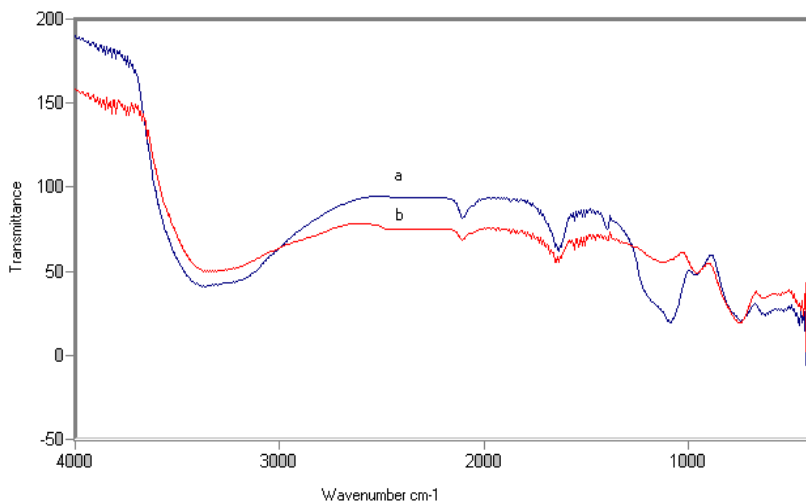


**Fig. 2.** IR-spectra of iron silico-antimonate with different antimony contents, FeSiSb-111 (a) and FeSiSb-114 (b).

DTA/TG thermograms shown in Fig. 3 (a & b) indicated that either FeSiSb (111) or FeSiSb (114) samples are thermally stable up to 900 °C and have nearly the same values of water content (20.20 and 20.65%, respectively). The water content was dehydrated in one endothermic DTA-peak with maximum at 88 °C in the case of FeSiSb (111). Where, in the case of FeSiSb (114), three simultaneous DTA-endothermic peaks at 112.9, 298 and 920 °C were obtained (Fig. 3b).

It is known that, the dehydration process against temperature may be belongs to the surface adsorbed water, mixed of crystalline and strongly bound water molecules present in interstices and to the loss of water during the condensation of surfaces hydroxyl groups<sup>18,19</sup>. In addition, Fig. 3b shows, new minor TG- mass loss accompanied with minor endothermic peak at ~ 980°C. This last peak of mass change appeared to increase in a slight mode with increasing the affective temperature which may be attributed to starting evaporation excess weight of antimony oxide of FeSiSb (114)<sup>20</sup>.

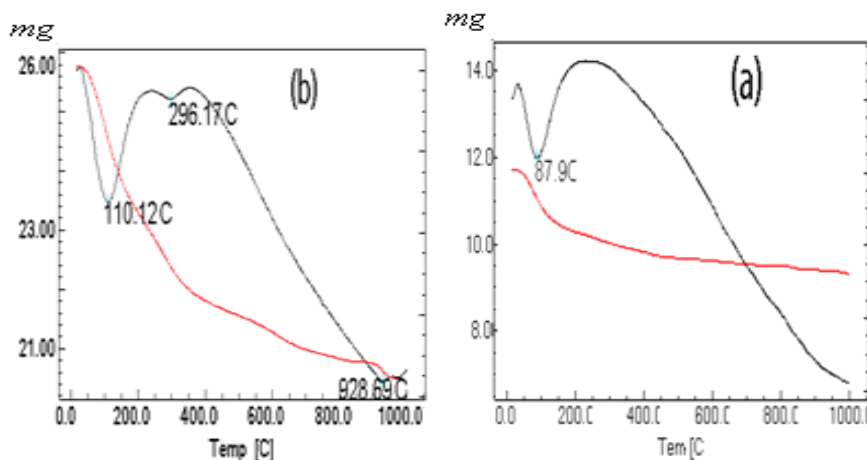
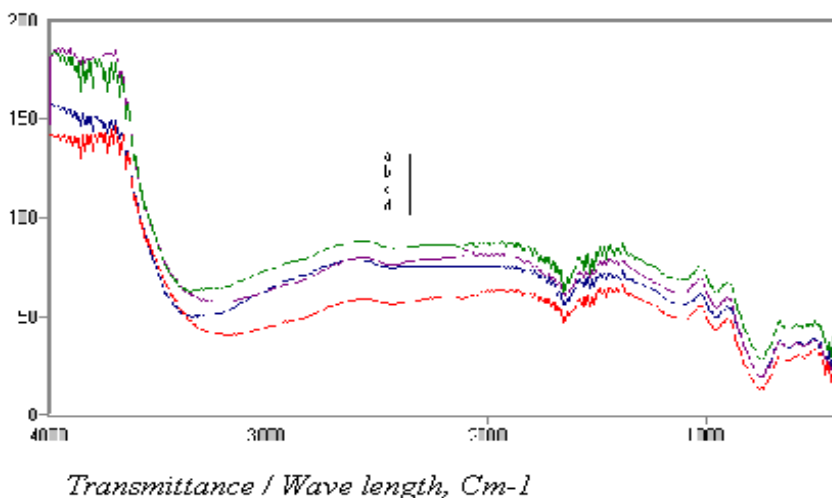


Fig. 3. DTA/TG thermograms of iron-antimonate, FeSiSb-111 (a) and FeSiSb-114 (b).

On the other hand, similar IR-spectra (Fig. 4) have been obtained for FeSiSb (114) samples that irradiated at 0, 25, 50 and 100 kGy. Some details such as water contents, color and ion exchange capacity are given in Table 1. All the previous data indicate that, iron silico-antimonates will have surface hydroxyl groups and thus become more available for the exchange with metal ions from aqueous media.



**Fig. 4.** IR spectra of iron silico-antimonate (FeSiSb-114) at different irradiated doses, 0 (a), 25 (b), 50 (c) and 100 kGy (d).

### *Ion exchange studies*

The ion exchange properties of the product materials were studied by measuring their distribution coefficients ( $k_d$ ) using batch experiments. Fig. 5 shows the variation of  $K_d$  values of  $10^{-3}$  M of  $\text{Sr}^{2+}$  and  $\text{Ce}^{3+}$  ions on FeSiSb (111) and (114) from nitric acid media. A linear relationship with a slope values lower than the valence of each sorbed ion was obtained on the two adsorbents from the nitric acid concentration range 0.01- 0.1M. Deviation of the obtained slopes from the valency of sorbed ions may be due to the participation of a mechanism other than ion exchange, like precipitation, surface adsorption, or simultaneous adsorption of anions<sup>21</sup>. Fig. 5 also shows that, the distribution coefficients for  $\text{Sr}^{2+}$  and  $\text{Ce}^{3+}$  ions were slightly increased with decreasing the acid concentrations ( $10^{-1}$ - $10^{-4}$  M). The increase in the ions removal with  $[\text{H}^+]$  decreasing can be explained on the basis of a decrease in competition between protons and positively charged metal ion at the surface sites, and by decrease in positive charge which results in a lower repulsion of adsorbing metal ion.

It is evident that the adsorption of metal ion decreases with increasing the acid concentration which is an obvious phenomenon. This is a common observation for all cases of adsorption of metal cations on solid surface from media of different acidity-basicity<sup>16,22,23</sup>. In our study, at high acidity, the



antimonate surfaces will be completely covered with  $\text{H}_3\text{O}^+$  ions and either  $\text{Sr}^{2+}$  or  $\text{Ce}^{3+}$  can hardly compete with proton for adsorption sites. This decrease in adsorption may be also explained in the light of two factors: (i) the decrease of water activity which is likely to be a mode of bridging in between solid/sorbate interface<sup>(24)</sup> and (ii) the excess of  $\text{H}^+$  ions compete for solid surface as compare to either  $\text{Sr}^{2+}$  or  $\text{Ce}^{3+}$  ions resulting in positively charged surfaces<sup>25</sup>. These two combined factors then would work for suppression of the adsorption of ions on each iron silico-antimonates.

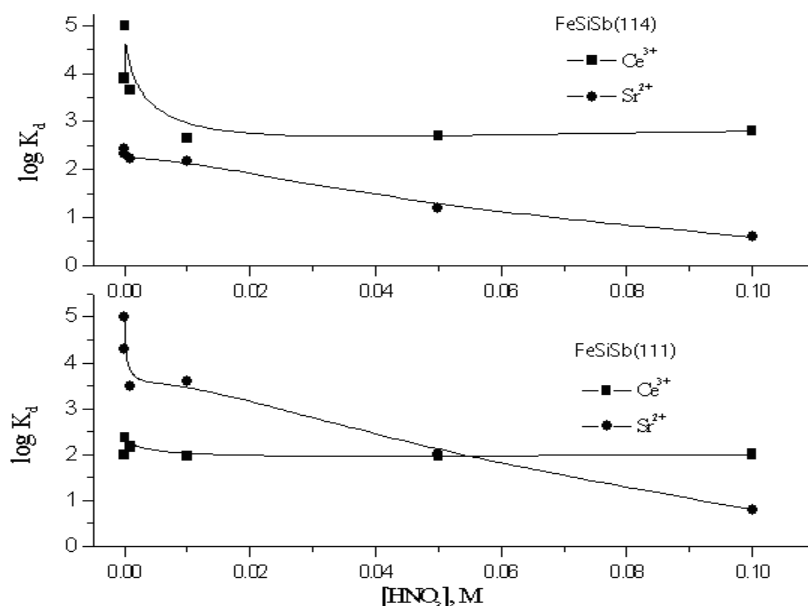


**Fig. 5.**  $\log K_d$  against  $[\text{HNO}_3]$  of  $\text{Sr}^{2+}$  and  $\text{Ce}^{3+}$  ions on FeSiSb (111) and FeSiSb (114) at  $25 \pm 1^\circ\text{C}$ .

On the other hand, an opposite selectivity order for each ions on the two exchangers was found in all acid concentrations. Hence, FeSiSb (111) with amorphous nature indicated the selectivity order  $\text{Sr}^{2+} > \text{Ce}^{3+}$  but the FeSiSb (114) indicated the order  $\text{Ce}^{3+} > \text{Sr}^{2+}$ . Different factors can affect on the selectivity of the ion exchange processes such as, hydrated ionic radii, ionic charge, hydration energy, structural hindrance and so on. According to the literature<sup>26</sup>, a low crystallinity or amorphous structure was favored because of its possible positive effects on the ion exchange properties of the materials. The ion exchange

properties of the synthesized iron silico-antimonates were surprisingly diverse. Over addition of antimony to the stoichiometric material FeSiSb (111) indicated substantial effect on the material, and their strontium and cerium uptake. However, because of phase changes with increasing  $\text{Sb}^{5+}$  content to produce the FeSiSb (114) with cubic structure (Fig. 1) no capacity or ions affinity decrease. Table 1 cleared that, the  $\text{Na}^+$  ion exchange capacity increased with phase transformation from amorphous FeSiSb (111) to cubic FeSiSb (114). This unexpected higher ions affinity of crystalline product may be related to the developing of acidity character of material due to the antimony content increasing which may be overcome on the crystalline nature<sup>27</sup>.

According to the above results, it seems that the excess in molar ratio of antimony will cause positive effect in producing the cubic phase of FeSiSb (114). Therefore, the highest  $K_d$  value that obtained on FeSiSb (114) via a maximum antimony substitution level (Fig. 5) may suggest that the electrostatic forces to be the dominant factor on the cerium uptake while the structural hindrance controlled the strontium exchange.

Also, from Fig. 5 it can be seen that, FeSiSb (114) is the higher sorption affinity toward  $\text{Ce}^{3+}$  ions compared to FeSiSb (111) at high acid concentrations. This observation may be related to the high acidity of the former exchanger due to the stoichiometric presence of  $\text{Sb}^{5+}$  as a major ion as well as its bigger ionic radii [ $\text{Sb}(0.76 \text{ \AA}) > \text{Fe}(0.65 \text{ \AA}) > \text{Si}(0.40 \text{ \AA})$ ] which support the efficiency of the antimonate matrix. Similar result was reported for the adsorption of cobalt ions on tin antimonates<sup>(26)</sup>. In addition, it was reported that, as the amount of  $\text{Sb}^{5+}$  increases the acidities of the material increase which leads to increasing the electrostatic interaction of the counter ions with the exchange sites<sup>(27)</sup>. This dependency indicated by the overall increase in  $K_d$  values in the case of FeSiSb (114). The last result may be generalized in preparing new inorganic ion exchange materials more effective in high acidic conditions.

Based on the results of batch distribution studies, binary separation of  $\text{Sr}^{2+}$ - $\text{Ce}^{3+}$  can be achieved on the different inorganic exchangers depending on the values of separation factors ( $K_a$ ) given in Table 3. At  $10^{-4} \text{ M } [\text{H}^+]$  the separation factor ( $K_a$ ) of  $\text{Sr}^{2+}$ - $\text{Ce}^{3+}$  was found equals 478 on FeSiSb (111) while it was found 1002 in the case of FeSiSb(114) at neutral condition. Thus, considering

the  $K_a$  values well suggest some separations which can be succeed especially in the case of nuclear fission products treatments.

**Table 3.  $K_d$  values and separation factors ( $K_a$ )\* of  $Sr^{2+}$  and  $Ce^{3+}$  ions on iron silico-antimonates at different acid concentrations.**

[H <sup>+</sup> ]	Distribution coefficients (ml/g)			
	FeSiSb(111)		FeSiSb(114)	
	Sr <sup>2+</sup>	Ce <sup>3+</sup>	Ce <sup>3+</sup>	Sr <sup>2+</sup>
0	270	1900 (7.0)*	100.0	99900 (1002)*
10 <sup>-4</sup>	209	99900 (478)*	230.0	19900 (86.5)*
10 <sup>-3</sup>	170	4445 (26)*	248.0	2280 (9.2)*
10 <sup>-2</sup>	153	376 (2.45)*	91.0	1566 (17.2)*
10 <sup>-1</sup>	4.0	809 (202)*	120.0	6.0 (0.05)*

\* represent the  $K_a$ , ( $K_{a\ Ce} = K_{d\ Ce}/K_{d\ Sr}$  or  $K_{d\ Sr} = K_{d\ Sr}/K_{d\ Ce}$ )

### *Effect of $\gamma$ - irradiation*

The diffractograms of the original and irradiated samples are rather similar. Comparison of the respective diffractograms recorded before and after irradiation enables us to conclude that, FeSiSb (114) did not change their original structure under the studied exposure doses (25-100kGy) of  $\gamma$ -radiation.

The same observation holds for the FeSiSb (114) as well: no change can be revealed between the thermograms (% water content and DTA peaks) of the original and its irradiated samples where there is no mass change or radiolysis takes place under  $\gamma$ - irradiation as given in Table 1.

The FT-IR spectra of the original and irradiated FeSiSb (114) are shown in Fig. 4. Figure 4 indicated that curves with the same characteristic bands before and after irradiation. The band characteristics for OH groups and Si atoms also seemed to be stable under the irradiation effect. Thus the IR-spectra proved that no chemical changes in the molecule takes place during the irradiation process under the given conditions.

Based on the above results, Fig. 6 shows the relation of the percent uptake of  $Sr^{2+}$  and  $Ce^{3+}$  ions against the irradiation doses of iron silico-antimonate. The figure clears that no changes in the adsorption performance of the two exchangers with increasing the  $\gamma$ - doses which support the suitability for use as ion exchanger up to the studied conditions. It is noteworthy that,

neglected increase in the ion uptake percent (Fig. 6) with increasing  $\gamma$ -doses. Thus, some radiolysis of the surface adsorbed water under irradiation may be occurred as may be notice from the thermogravimetric data of irradiated samples given in Table 1. Iron silico-antimonate sorbents evidently can withstand even higher doses, which makes them extremely promising for reprocessing high-activity wastes.

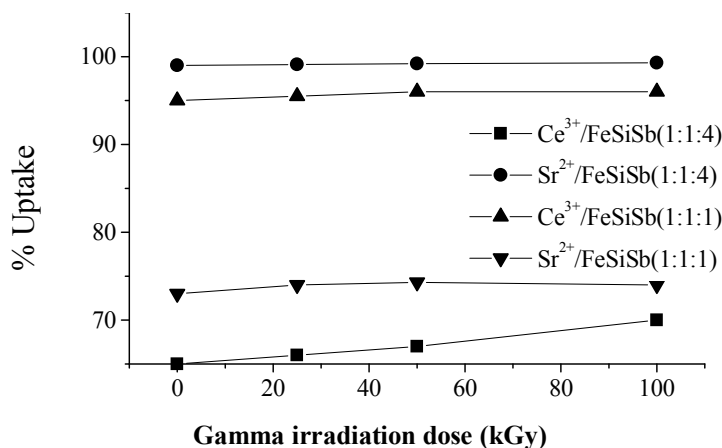


**Fig. 6.** Effect of gamma irradiation doses on the % uptake of  $\text{Sr}^{2+}$  and  $\text{Ce}^{3+}$  ions on FeSiSb (111) and FeSiSb (114) at neutral pH and  $25 \pm 1^\circ\text{C}$ .

### *Effect of the reaction temperature*

The adsorption of strontium or cerium ions on each of FeSiSb (111) or FeSiSb (114) in the temperature range  $293\text{--}333\text{K}^\circ$  at constant initial concentrations of  $10^{-3}\text{M}$  of metal ions in aqueous solution at pH 5.4 are studied. However, temperature influences both the rate and the amount uptake, but the time required to attain the adsorption equilibrium remains almost unchanged. The uptake amounts at equilibrium for the various temperatures are listed in Table 4. Table 4 shows that the amount uptake increases with the increase in temperature from  $293$  to  $333\text{K}^\circ$  in the case of FeSiSb (114) while in the case of FeSiSb (111), there is slightly decrease with increasing the reaction temperatures. The increase in the amount uptake at equilibrium with temperature (endothermic process) may be either due to creation of some active

sites on the adsorbent surface or due to acceleration of some originally very slow adsorption steps<sup>28</sup>.

**Table 4. Values of thermodynamic parameters and amount uptake of Sr<sup>2+</sup> and Ce<sup>3+</sup> ions on iron silico-antimonates.**

Exchanger	ion	$\Delta H^\circ$ , kJ/mol	$\Delta S^\circ$ , J/k/ mol	$-\Delta G$ (kJ/ mol)			Amount uptaken, (mol g <sup>-1</sup> ) x 10 <sup>5</sup>		
				293	313	333	293	313	333
FeSiSb (111)	Sr <sup>2+</sup>	-11.0	9.76	13.6	14.1	14.2	7.30	7.00	6.30
	Ce <sup>3+</sup>	-17.3	4.21	18.2	18.3	18.8	9.48	9.20	9.00
FeSiSb (114)	Sr <sup>2+</sup>	48.9	110.2	28.0	31.7	38.2	9.99	9.99	9.99
	Ce <sup>3+</sup>	19.2	103.4	12.7	14.0	15.0	6.50	6.72	6.94

On the other hand, parameters like free energy change ( $\Delta G^\circ$ ), enthalpy change ( $\Delta H^\circ$ ), and entropy change ( $\Delta S^\circ$ ) were estimated using the following equations. The Gibb's free energy change of the process is related to the distribution coefficient ( $K_d$ ) by the equations:

$$\Delta G^\circ = -RT \ln K_d \quad (4)$$

$$\Delta G^\circ = \Delta H^\circ - T\Delta S^\circ \quad (5)$$

$$\log K_d = \Delta S^\circ / 2.303R - \Delta H^\circ / 2.303RT \quad (6)$$

where;  $K_d$  is the distribution coefficient (ml/g), and  $R$  is gas constant (kJ mol<sup>-1</sup> K<sup>-1</sup>). According to the last equation given above the values of  $\Delta H^\circ$  and  $\Delta S^\circ$  can be calculated from the slopes ( $\Delta H^\circ / 2.303R$ ) and intercepts ( $\Delta S^\circ / 2.303R$ ) of  $\log K_d$  versus  $1/T$  plots as shown in Fig. 7. The calculated values of thermodynamic parameters were given in Table 4. As it can be seen from Table 4,  $\Delta H$  values are found to be positive for Sr(II) and Ce(III) sorption on FeSiSb (114) matrix. These positive values assigned to the endothermic nature of the sorption process. Although there are no certain criteria related to the  $\Delta H^\circ$  values that define the adsorption type, the values of heat of adsorption are 48.96 and 19.21 kJ mol<sup>-1</sup>. These values are frequently assumed as the comparable values for the chemical adsorption processes<sup>(27)</sup>. For FeSiSb (111),  $\Delta H$  values were found to be -11.02 and -17.31 kJ mol<sup>-1</sup> for Sr(II) and Ce(III) ions, respectively. It is obvious from the obtained  $\Delta H^\circ$  values that ion exchange mechanism takes place in the adsorption process.

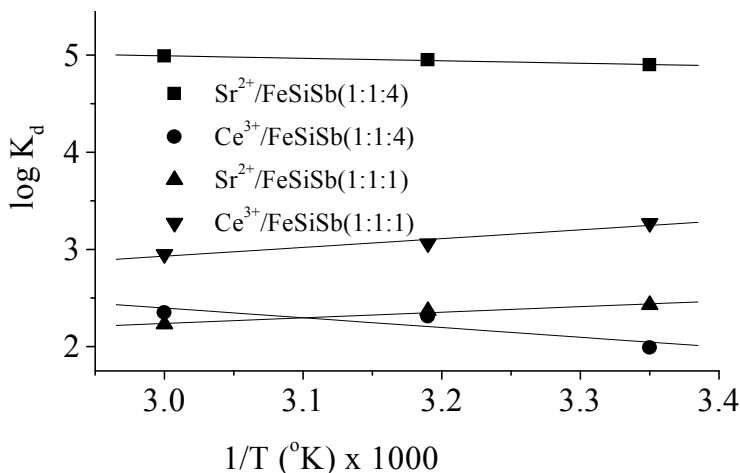


**Fig. 7. Variation of  $\log K_d$  vs  $1/T$  for adsorption of Sr(II) and Ce(III) on iron silico-antimonate in different structures (initial concentration  $1.0 \times 10^{-3} \text{ M}$ ; pH neutral).**

Negative values of Gibbs free energy  $\Delta G$ , for the exchange of Sr(II) and Ce(III) ions on two antimonate phases indicate the spontaneous nature of the reactions. It is possible to say that the adsorptive forces are strong enough to break the potential and shift the reaction ultimately to the right leading to bending of  $\text{Sr}^{2+}$  or  $\text{Ce}^{3+}$  onto surface constituents of both exchangers. In addition, the increase in negative Gibbs free energy with increasing the reaction temperature means the reaction is favored and getting easier at higher temperatures. The values of  $\Delta S$  were found to be positive in all cases due to the exchange of the metal ions with more mobile ions present on the exchanger. The positively  $\Delta S$  would cause increase in the entropy (increase randomness), during the adsorption process especially in the case of FeSiSb (114) exchanger. In this concern, in the case of physico-sorption which may also contribute to the total adsorption process can cause increase in entropy. This is because of the water molecules released from the hydrated ions or water molecules present on the surface during the adsorption process <sup>(29)</sup>.

## CONCLUSION

Two new synthesized forms of incorporating iron oxide- silicoantimonate was studied as inorganic ion exchangers with higher chemical, mechanical and radiation stabilities due to iron presence. The obtained materials indicated that, phase transformation to higher crystalline nature due to  $\text{Sb}^{5+}$  increasing. Also

these materials indicated higher acidity with increasing in Sb content which reinforces its application as ion exchanger in acidic environment. The distribution and selectivity performance of Sr (II) and Ce (III) ions on each antimonate forms have been studied at different acid concentration, irradiation doses and reaction temperature. Different selectivity trend was obtained for the two exchangers at lower acid concentrations.

## REFERENCES

1. Siddiqi, Z., Pathania, D. (2003) Studies on titanium (IV) tungstosilicate and titanium (IV) tungstophosphate. II. separation and estimation of heavy metals from aquatic environments. *Acta Chromatographia*, 13, 172.
2. Mittal, S., Sharma, H., Kumar, S. (2006) Synthesis, characterization and analytical application of zirconium (IV) antimonate as a potentiometric sensor. *React. & Func. Polym.*, 66, 1174.
3. Nabi, S. and Khan, A. (2006) Synthesis, ion exchange properties and analytical applications of stannic silicomolybdate: Effect of temperature on distribution coefficients of metal ions. *Reactive & Functional Polymers*, 66, 495.
4. Nabi, S. and Naushad, Mu. (2007) Inamuddin, Synthesis and characterization of a new inorganic cation - exchanger - Zr (IV) tungstomolybdate. *J. Hazard. Mats*, 142, 404.
5. Nabi, S., Shalla, A., Khan, A. and Ganie, S. (2007) Synthesis, characterization and analytical applications of titanium (IV) molybdatesilicate. *Coll. & Surfs*, 302, 241.
6. H. Kaneko, M. Abe, T. Tsuji, Y. Tamaura, Ion-exchange selectivity and chromatographic separation of trivalent metals on titanium antimonate. *Chromatographia*, 35, (1993) 183.
7. Burham, N., Abdel-Halim, S., El-Naggar, I., El-Shahat, M. (1995) Synthesis and characterization of tin(IV)antimonate and study of its ion-exchange equilibria. *J. Radioanal. & Nucl. Chem.* 189 (1), 183.
8. Aly, H., El-Naggar, I. (1998) Synthesis of tetravalent metal antimonates: Characteristics and use in treatment of radioactive waste solutions. *J. Radioanal. & Nucl. Chem.* 228, 151.
9. El-Naggar, I., Abdel-Hamid, M., Shady, S. and Aly, H. (1995) Radioactive Waste Managements Environmental Radiation, ASME, Germany.

10. Möller, T., Harjula, R., Kelokaski, P., Vaaramaa, K., Karhu, P. and Lehto, J. (2003) Titanium antimonates in various Ti:Sb ratios: ion exchange properties for radionuclide ions. *J. Mater. Chem.* 13, 535.
11. Varshney, K., Sharma, U. (1985) Kinetics of ion-exchange of transition metals on tin (IV) arsenosilicate cation exchanger. *J. Reac. Kints & Cata. Letts.* 28, 28.
12. Mittal, S., Nath, R. and Banait, J. (2007) New method of synthesis of stannic phosphotungstate and its characterization as ion exchanger. *J. Chemistry*, 1,1.
13. Khan, A., Alam, M., and Mohammad, F. (2003) Ion-exchange kinetics and electrical conductivity studies of polyaniline Sn(IV) tungstoarsenate; a new semi-crystalline 'polymeric-inorganic' composite cation-exchange material. *Electrochimica Acta*, 48, 2463.
14. Thakkar, R. and Chudasama, U. (2007) Synthesis, Characterization and thermodynamics of exchange using zirconium titanium phosphate cation exchanger. *Collection of Czechosl. Chem. Communics*, 72, 1306.
15. Card (1995) 33-1018, Joint Committee on Powder Diffraction Standards JCPDS- ICDD, USA.
16. Ali, I., Zakaria, E., Ibrahim, M. and El-Naggar, I. M. (2008) Synthesis, structure, dehydration transformations and ion exchange characteristics of iron-silicate with various Si and Fe contents as mixed oxides. *Polyh.* 27, 429.
17. Rao, C. (1963) Chemical applications of infrared spectroscopy, Academic Press, New York.
18. Duval (1963) Inorganic Thermogravimetric Analysis, Elsevier, Amsterdam.
19. Sivaiah, M., Venkatesan, K., Sasidhar, P., Krishna, R. (2004) Ion exchange studies of cerium (III) on uranium antimonite. *J. Nucl. & Radiochem. Scis*, 5, 7.
20. Subramanian, M., Clearfield, A., Umarji, A., Shenoy, G. and Rao, G. (1984) Synthesis and solid state studies on  $\text{Mn}_2\text{Sb}_2\text{O}_7$  and  $(\text{Mn}_{1-x}\text{Cd}_x)_2\text{Sb}_2\text{O}_7$  pyrochlores. *J. Solid State Chem.* 52, 124.
21. Hefferich, F. (1962) ion Exchange, McGraw-Hill, New York,
22. Padmavathy, V., Vasudevan, P. and Dhingra, S. (2003) Proc. Biochem., Biosorption of nickel (II) ions on Baker's yeast, 38, 1389.



23. Ali, I. M. (2003) Synthesis and sorption behavior of semicrystalline sodium titanate as a new cation exchanger. *J. Radioanal. & Nucl. Chem.* 260, 149.
  24. Hasany, S. M. Chaudhary, M. H. (1981) Adsorption studies of strontium on manganese dioxide from aqueous solutions. *Appl. Radiat. Isot.* 32, 899.
  25. Mishra, S., Singh, V. and Tiwari, D. (1997) Radiotracer technique in adsorption study XVI, Efficient removal of cadmium ions by sodium titanate from aqueous solution. *Appl. Radiat. Isot.* 48, 435.
  26. Koivula, R., Harjula, R. and Lehto, J. (2002) Structure and ion exchange properties of tin antimonates with various Sn and Sb contents. *Micropours & Mesopours Mats*, 55, 231.
  27. Moller, T., Harjula, R., Pillinger, M., Dyer, A., Newton, J., Tusa, E., Amin, S., Webbe, M. and Arayae, A. (2001) Uptake of  $^{85}\text{Sr}$ ,  $^{134}\text{Cs}$  and  $^{57}\text{Co}$  by antimony silicates doped with  $\text{Ti}^{4+}$ ,  $\text{Nb}^{5+}$ ,  $\text{Mo}^{6+}$  and  $\text{W}^{6+}$ . *J. Mater. Chem.* 11, 1526.
  28. Mishra, S., and Tiwari, D. (1991) Ion exchange in radioactive waste management, part VIII, Radiotracer studies on adsorption of strontium ions on hydrous manganese oxide. *Appl. Radiat. Isot.* 42, 1177.
  29. Unlu, N., Ersoz, M. (2006) Adsorption characteristics of heavy metal ions onto a low cost biopolymeric sorbent from aqueous solutions. *J. Hazards Mats*, 136, 272.
-



## مجلة البحوث الإشعاعية والعلوم التطبيقية

مجلد 1 عدد 2 ص ص 261 – 278 (2008)

### دراسة تكوين وخواص وتأثير أشعة جاما على السلوك الأمتصاصي لمبادل حديد سيليكوانتيمونات

إسماعيل محمد على و عصام صالح زكريا و إبراهيم النجار

مركز المعامل الحارة- هيئة الطاقة الذرية- ص ب 13759 - القاهرة- مصر.

في هذا البحث تم تحضير مركب الحديد سيليكوانتيمونات في حالتين مختلفتين وذلك باستخدام نسب مولارية مختلفة من السليكون والأنتيمون. وقد تم دراسة التركيب والخواص الفيزيوكيميائية للمركبين المحضرين باستخدام الأجهزة التحليلية المتقدمة، وقد وجد أنهما يمتازان بثبات كيميائي بالإضافة إلى تحملها لدرجات حرارة وجرعات إشعاعية عالية. وتم دراسة معامل التوزيع وسعة التبادل الأيوني لبعض العناصر ذات الأهمية النووية مثل الأسترونشيوم والسير يوم وتبين أن المركبين لهما قدرة فصل ومعالجة جيدة عند درجات الحموضة الأقل وكذلك زيادة تلك القدرة بزيادة نسبة الأنتيمون في المركب، وقد تم أيضا دراسة تأثير جرعات مختلفة من إشعاع جاما على المركب الأعلى في نسبة الأنتيمون ووجد أن له درجة ثبات عالية سواء في الخواص الفيزيائية والتركيب أو في سعة التبادل الأيوني. أيضا تم دراسة تأثير درجة حرارة التفاعل على عملية الاتزان وأمكن حساب بعض دوال الديناميكا الحرارية لعملية التبادل الأيوني. وهذه الدراسة من الدراسات المهمة والواعدة في تكنولوجيا معالجة المخلفات المشعة السائلة باستخدام مواد محضرة خصيصا لعمليات الفصل.